Temperature dependent distinct coupling and dispersions of heavy- and light-hole excitonic polaritons in ZnO

C. C. Zheng,[1,2] S. J. Xu,[1,a)] J. Q. Ning,[1] Y. N. Chen,[1,b)] F. Zhang,[1] and C. M. Che[2]
[1]*Department of Physics and HKU-CAS Joint Laboratory on New Materials, The University of Hong Kong, Pokfulam Road, Hong Kong, China*
[2]*Department of Chemistry, Institute of Molecular Functional Materials, HKU-CAS Joint Laboratory on New Materials, The University of Hong Kong, Pokfulam Road, Hong Kong, China*

Distinct coupling behavior of heavy- and light-hole excitonic polaritons in ZnO was unveiled by investigating the optical reflectance spectra of a high quality ZnO single crystal as a function of temperature both experimentally and theoretically. A resonance like coupling region was found at a temperature of around 50 K at which several relevant physical quantities such as the transverse exciton transition energy, polarizability, and damping parameters of the two kinds of excitonic polaritons were revealed to overturn. Calculated dispersions correctly reflect the nature of coupled photon and exciton and reproduce the spectral structures of the interacting polaritons. © *2012 American Institute of Physics*. [http://dx.doi.org/10.1063/1.4722933]

In recent years, ZnO and its nanostructures have attracted a great deal of interest due to its outstanding properties and potential applications in optoelectronic devices, piezoelectric devices, ultraviolet diodes/detectors, solar cells, and spintronic devices.[1–4] Exploiting these potential device applications of ZnO certainly requires a good understanding of fundamental elemental excitations such as excitons, polaritons, polarons as well as their interactions in ZnO.[5–9] It is known that polariton is a composite quasiparticle of exciton and photon, possessing the dual nature of half-particle and half-wave. It has a profound influence on the optical properties of solids, especially semiconductors.[5,6] Optical reflectance spectrum has been demonstrated to be a powerful tool for studying the polariton effects because it is free from the relaxation problem.[10] In wurtzite ZnO, two kinds of excitonic polaritons associated with heavy- and light-hole excitons, respectively, could exist due to the crystal field induced valence band splitting, namely Γ_7 and Γ_9 bands. The symmetry ordering of these two split valance bands, that is which one is the uppermost band, was an unsettled problem for many years.[5,9,11] Very recently, some comprehensive low-temperature magneto-photoluminescence spectral data of the bound excitonic transitions in high quality ZnO crystals have provided strong evidence for the statement of the Γ_7 symmetry of the uppermost valance band.[9,12] The two kinds of excitonic polaritons related to the two valance bands may have strong coupling in ZnO due to the small energy separation of ~5 meV between them, especially in a temperature range in which the thermal energy is close to this energy separation. In the past, only the low-temperature optical reflectance spectra of ZnO were reported.[5,6,8,13] Therefore, a detailed study on variable-temperature optical reflectance spectra of ZnO, especially on possible strong coupling behavior of the two kinds of excitonic polaritons in ZnO is interesting and might be significant.

In this letter, we present a combined study of experiment and theory on the variable-temperature reflectance spectra of the interacting heavy- and light-hole excitonic polaritons in a high-quality ZnO single crystal. Interesting mixing behavior of the two kinds of excitonic polaritons against temperature was revealed both experimentally and theoretically. Some relevant physical quantities such as the transverse exciton transition energy, polarizability, and damping parameters of both the excitonic polaritons show a unified distinct behavior against temperature, that is, "flipping" behavior beyond about 50 K.

The sample used in this study was a high-quality ZnO single crystal (Cermet, Inc.) with a thickness of 0.5 mm. It was synthesized by melt grown method and polished on its c-plane (Zn-terminating face). Its optical and crystalline quality was well confirmed by low temperature photoluminescence spectrum which shows intensive and sharp band-edge excitontic emissions and almost no impurity/defect related visible emission (not shown here). The optical reflectance spectrum measurements were carried out under the geometric configuration of almost normal incidence (~10° departure from the c-axis of the sample). The incident monochromatic light was obtained by dispersing the white light of the xenon lamp using a monochromator (Acton SP305) equipped with a 1200 grooves/mm grating. The scanning step of the monochromator was set to 0.05 nm during the measurements. The reflectance signal from the sample was detected by a Hamamatsu silicon *p-i-n* photodiode. For the variable-temperature reflectance spectrum measurements, the sample was mounted on the cold finger of a Janis closed cycle cryostat (CCS-150) with a varying temperature range from 9 to 300 K. The reflectance spectra were registered in a wavelength range of 355–375 nm where the excitonic polariton transitions took place.

Figure 1 shows the optical reflectance spectra (the empty scatters for the experimental spectra and the solid lines for the theoretical curves) from the ZnO single crystal at several different temperatures. From Fig. 1, the double structures in

a)Author to whom correspondence should be addressed. Electronic mail: sjxu@hku.hk.
b)Present address: Laboratoire "Materiaux et Phenomenes Quantiques," Universite Paris Diderot-Paris 7, 75013 Paris, France.
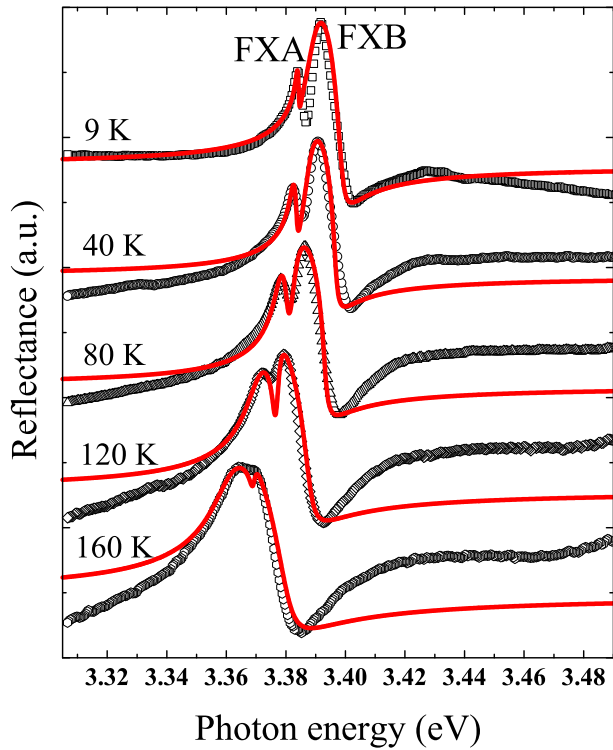
100, 221105-1

FIG. 1. Reflectance spectra of a high quality ZnO single crystal at some representative temperatures (in different shapes of empty scatters) together with the corresponding theoretical curves (in solid lines) calculated by an interacting polariton model.

the reflectance spectra are close to each other but well resolved in the interested temperature range from 9 K to 160 K. They doubtlessly correspond to the heavy- and light-hole excitonic polaritons that are denoted as FXA and FXB, respectively, just for the simplicity. The spectral structure is extraordinary, i.e., significant spectral overlapping of the FXA and FXB peaks and the dominance of FXB located at higher energy. Such spectral structure of ZnO is different from that of GaN that has the same wurtzite structure and similar band structures as ZnO.[14] More interestingly, this unusual spectral structure exhibits a distinct evolution behavior upon temperature. At low temperatures, the peculiarly strong of FXB peak which is in contrast to the case of GaN[14] indicates unusual ordering of the uppermost valence bands in ZnO. As mentioned in the introduction part, recent precise low-temperature magnetophotoluminescence experiments show strong evidence that the top valance band has the Γ_7 symmetry.[9,12] In other words, the topmost valence band is light-hole band rather than heavy-hole band in ZnO at low temperatures. The larger effective mass and thus effective density of states of heavy hole makes the relative intensity of FXB extraordinarily strong. Indeed, our low-temperature reflectance spectra favor such statement. However, the relative intensities of FXA and FXB flip up for the temperature beyond 150 K, which means that the ordering of the uppermost valence bands in ZnO returns to the normal configuration at higher temperatures. These spectral features and their distinct temperature dependence are very interesting and need to be elucidated carefully. To do so, the interacting excitonic polariton model considering two polariton branches was adopted to calculate the theoretical reflectance

spectra of ZnO.[15] In this model, the dielectric function can be written as[14–16]

$$\varepsilon(k,\omega) = \varepsilon_b + \frac{4\pi\beta_A\omega_{0A}^2}{\omega_{0A}^2 - \omega^2 + \hbar k^2\omega_{0A}/M_A - i\Gamma_A\omega}$$
$$+ \frac{4\pi\beta_B\omega_{0B}^2}{\omega_{0B}^2 - \omega^2 + \hbar k^2\omega_{0B}/M_B - i\Gamma_B\omega}, \quad (1)$$

where ε_b is the wave vector independent background dielectric constant, k the wave vector, $\omega_{0A(B)}$ the resonance frequency/energy of FXA(B), $M_{A(B)}$ the total effective mass of the heavy-hole (light-hole) exciton, m_e and $m_{h(l)h}$ the effective masses of electrons and heavy (light) holes, respectively, $\Gamma_{A(B)}$ the damping parameter (wave vector independent) which describes the various scattering processes such as impurity and/or phonon scattering,[14,17–19] and $4\pi\beta_{A(B)}$ the polarizability of FXA(B). The details for calculating reflectivity at normal incidence from the dielectric constant described by Eq. (1) can be found in Ref. 14. Overall, good agreement between theory and experiment is achieved in the interested temperature range, as shown in Fig. 1. Agreement at lower temperatures is better than at higher temperatures. The deviation at higher temperatures for E > 3.39 eV is mainly due to the exclusion of C exciton associated with the spin-orbital band and its increase with temperature. The disagreement for E < 3.34 eV is likely caused by the change of the unknown background with temperature.

It is known that the polarizability of exciton is related to the longitudinal-transverse exciton energy difference that can be expressed as[10,20,21]

$$\Delta_{LT} = E_L - E_T = \frac{2\pi\beta E_T}{\varepsilon_b}, \quad (2)$$

where E_L and E_T are the longitudinal and transverse exciton energies, respectively. For the theoretical calculations of the reflectance spectra at different temperatures in the present work, $\varepsilon_b = 3.7$, $M_A = 0.83\,m_0$ for the light hole, and $M_B = 1.04\,m_0$ for the heavy hole (m_0 is the free electron mass) were adopted and kept unchanged against temperature,[1] while the remaining parameters were adjustable for different temperatures. Considering the reversed order of the heavy- and light-hole bands in ZnO at low temperatures and the difference in the effective mass between them, we adopted a recently determined heavy-hole effective mass $m_{hh} = 0.8\,m_0$ in ZnO,[22] while the light-hole effective mass was taken from Ref. 1. It should be noted that the effective mass was verified to be no significant impact to the theoretical reflectance spectra and dispersions of interacting polaritons. Within the scope of this work, the transverse modes were calculated using the condition

$$\varepsilon(k,\omega) = k^2 c^2/\omega^2, \quad (3)$$

where c is the light speed in the free space. Together with Eq. (1), a cubic equation of k^2 as a function of ω is given. Solving this cubic equation will generate the dispersion relation of the transverse modes. The solutions are complex functions considering damping, so only the real parts of the solutions are accepted (Re$[\sqrt{k^2}]$). In order to calculate the

theoretical reflectance curves, the additional boundary conditions (ABCs) proposed by Hopfield and Thomas who assumed that the excitonic polarizability should vanish at the surface were adopted.[14,23] It should be mentioned that only the transverse resonance energy can be directly extracted from the fitting of reflectance spectra, while the longitudinal resonance energy needs to be calculated from Eq. (2).

The resonance energies of FXA and FXB vs. temperature unveiled by the theoretical reflectance simulations show an outstanding agreement with the prediction from the Varshni formula,[24] as shown in Fig. 2. The symbols represent the experimental data while the solid lines are the fitting curves with the Varshni's formula whose expression was given in the figure. As pointed out and commented in a latest review article,[25] the temperature dependence of the band gap of semiconductors including ZnO can be fitted with the Varshni's empirical formula in which one of the two key parameters is closely related to the Debye temperature of the investigated material. The results presented in this work verify this conclusion again.

The calculated polariton dispersion curves from Eqs. (1) and (3) by adopting the values of the parameters obtained from the simulated reflectance curves at 9, 40, and 80 K are shown in Fig. 3. It should be noted that by combining Eqs. (1) and (3), a cubic equation of k^2 as a function of ω is yielded, whose roots are usually complex numbers. In our calculations, we get the square root of complex k^2 first, and then fetch the real part of this complex value, finally calculate the dispersion curves. In literature, however, the real part of complex k^2 was obtained first, and then the square root of this real part was yielded, and finally the dispersions were calculated.[8,13,14] From both mathematic and physical points of view, the latter approach is not appropriate. The excitonic polariton dispersions calculated by the latter approach cannot reflect the photon dispersion at vicinity $k = 0$ correctly. In contrast to the previous results, our results, i.e., the upper polariton branch of FXB (UPB_B) exactly shows the nature of both dispersion characteristics of photon and exciton. Furthermore, the coupling between photon and exciton as well as the interactions of FXA and FXB can be clearly seen in our results, as evidenced by the presence of
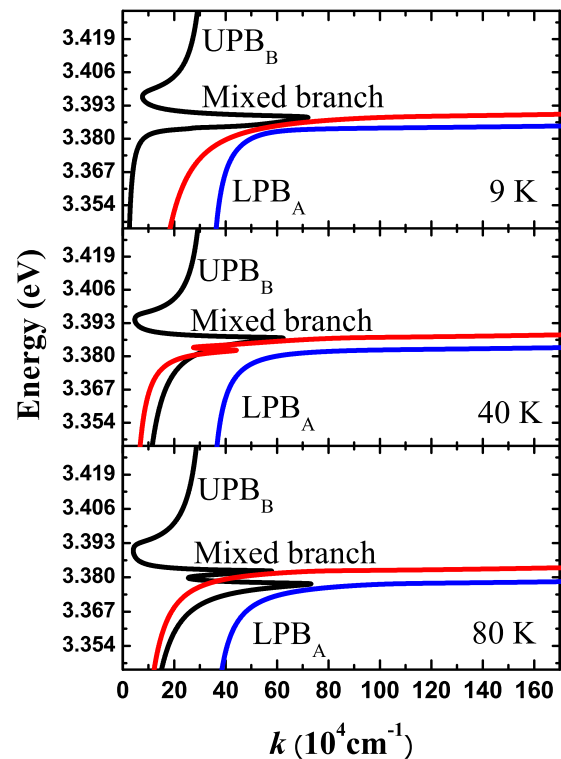
FIG. 3. Calculated dispersion relations of excitonic polariton A and B in ZnO using parameters of the 9, 40, and 80 K reflectance spectrum simulation. The upper, mixed, and lower branches are shown.

crossing behaviors due to the nature of the interacting polariton model. In Fig. 3, three branches of polaritons, namely upper polariton band B (UPB_B), mixed lower polariton band B (LPB_B)-upper polariton band A (UPB_A), and lower polariton band A (LPB_A), were depicted for the three temperatures. As expected, these dispersion curves clearly reflect the nature of coupled photon and exciton. For example, UPB_B and UPB_A show more photon-like properties at $k \approx 0$ while LPB_B and LPB_A exhibit more exciton-like properties for k taking large values. In the mixing region, depending on temperature, LPB_B and UPB_A mix and even cross. Also in this region, the dispersions can reproduce the main structure of the experimental reflectance spectra at different temperatures. At 9 K, one dominant peak associated with FXB appears in the LPB_B branch. At 80 K, clear double structures with comparable intensities can be seen in the dispersions. At 40 K, strong mixing occurs in the LPB_B and UPB_A dispersions. This implies that the strongest coupling between polariton A and B takes place at temperatures of 40–50 K. Interestingly, the energy splitting ($\Delta E_{AB} = \sim 5$ meV) of heavy- and light-hole excitonic polaritons is close to the thermal energy ($1.5 k_B T$) at around 50 K. Further evidence for the thermally induced resonant coupling between the two kinds of polaritons was obtained by analyzing the polarizability and damping parameters of FXA and FXB described below.

The polarizability of FXA and FXB vs. temperature is shown in Fig. 4(a). It is found that the polarizability of FXA increases with increasing temperature whereas the FXB's decreases. At around 50 K, the polarizability of FXA and FXB intersects. As the temperature goes up beyond this temperature, the polarizability of FXA and FXB tends to departure from each other again. Such temperature dependence
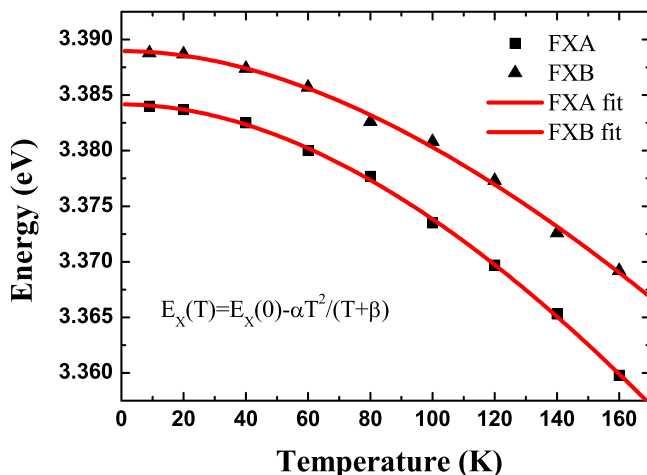

FIG. 2. Resonant energies (solid symbols) of FXA and FXB at different temperatures together with the fitting curves (solid lines) using the Varshni's formula, respectively.
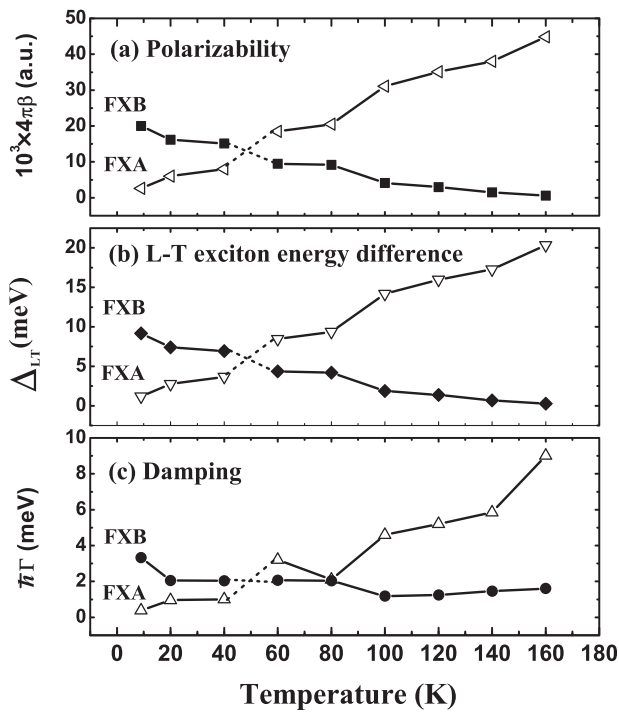
FIG. 4. Polarizability (a), longitudinal-transverse exciton energy difference (b), and damping (c) of FXA and FXB revealed by the calculations as a function of temperature. Dotted lines are used to connect the data within the mixing region.

behavior of the polarizability indicates the existence of a strong mixing region between FXA and FXB. Very similar behavior was also found for the longitudinal-transverse (L-T) exciton energy difference of FXA and FXB calculated from Eq. (2) using the transverse resonance energies and polarizabilities acquired from the theoretical simulations of the measured reflectance spectra, as shown in Fig. 4(b). The L-T splitting at 9 K is 1.19 and 9.16 meV for FXA and FXB, respectively, that is in agreement with the values reported by Lagois and Hümmer.[6] It is known that the longitudinal resonance energy reflects the energy of the interacting exciton and photon (polariton) at $\vec{k} = 0$, whereas the transverse resonance energy shows the energy of $\vec{k} = 0$ exciton in the limit of zero exciton-photon interaction.[19] Therefore, the exciton-photon coupling or polariton effect is prevailing for FXB at low temperatures. However, it weakens gradually for FXB as the temperature goes up. For FXA, the situation is just reverse. As a consequence, the polariton effect on FXA and FXB crosses at a temperature of around 50 K. As for the damping parameters of FXA and FXB shown in Fig. 4(c), they also exhibit distinct dependence on temperature. In the interested temperature range in the present study, the damping of FXB is larger at low temperatures and does not show a strong dependence on temperature, which can be attained to the impurity scattering. The damping of FXA increases linearly with temperature, reflecting the characteristic of the acoustic-phonon scattering.[26] The damping parameters of FXA and FXB also crosses at around 50 K.

In summary, the variable-temperature optical reflectance spectra of a high quality ZnO single crystal were measured and calculated with an interacting excitonic polariton model. At low temperatures, the relative intensity of FXB located at higher energy is peculiarly strong. But its relative intensity decreases with temperature and becomes eventually smaller than that of FXA. The excitonic resonance energies, polarizability, and damping parameters of the two kinds of excitonic polaritons associated with the valance bands A and B were found to show a "crossing" behavior when the temperature is beyond ∼50 K. The calculated dispersions of coupled polaritons support the experimental results. These findings not only enhance the existing understanding of the excitonic polaritons in ZnO but also help clarify the reversed ordering problem of the valance bands in ZnO at low temperatures.

[1]B. K. Meyer, H. Alves, D. M. Hofmann, W. Kriegseis, D. Forster, F. Bertram, J. Christen, A. Hoffmann, M. Strassburg, M. Dworzak, U. Haboeck, and A. V. Rodina, Phys. Status Solidi B **241**, 231 (2004).
[2]Ü. Özgür, Y. I. Alivov, C. Liu, A. Teke, M. A. Reshchikov, S. Dogan, V. Avrutin, S. J. Cho, and H. Morkoç, J. Appl. Phys. **98**, 041301 (2005).
[3]H. Morkoç and Ü. Özgür, *Zinc Oxide: Fundamentals, Materials and Device Technology* (WILEY-VCH, Weinheim, 2009).
[4]Z. L. Wang, J. Phys.: Condens. Matter. **16**, R829 (2004).
[5]J. J. Hopfield, J. Phys. Chem. Solids **15**, 97 (1960).
[6]J. Lagois and K. Hümmer, Phys. Status Solidi B **72**, 393 (1975).
[7]S. J. Xu, S. J. Xiong, and S. L. Shi, J. Chem. Phys. **123**, 221105 (2005).
[8]J. Fryar, E. McGlynn, M. O. Henry, and J. P. Mosnier, Nanotechnology **16**, 2625 (2005).
[9]M. R. Wagner, J. H. Schulze, R. Kirste, M. Cobet, A. Hoffmann, C. Rauch, A. V. Rodina, B. K. Meyer, U. Roder, and K. Thonke, Phys. Rev. B **80**, 205203 (2009).
[10]R. Stepniewski, K. P. Korona, A. Wysmolek, J. M. Baranowski, K. Pakula, M. Potemski, G. Martinez, I. Grzegory, and S. Porowski, Phys. Rev. B **56**, 15151 (1997).
[11]D. C. Reynolds, D. C. Look, B. Jogai, C. W. Litton, G. Cantwell, and W. C. Harsch, Phys. Rev. B **60**, 2340 (1999).
[12]L. Ding, B. K. Li, H. T. He, W. K. Ge, J. N. Wang, J. Q. Ning, X. M. Dai, C. C. Ling, and S. J. Xu, J. Appl. Phys. **105**, 053511 (2009).
[13]M. Cobet, C. Cobet, M. R. Wagner, N. Esser, C. Thomsen, and A. Hoffmann, Appl. Phys. Lett. **96**, 031904 (2010).
[14]Y. J. Wang, R. X. Wang, G. Q. Li, and S. J. Xu, J. Appl. Phys. **106**, 013514 (2009).
[15]J. Lagois, Phys. Rev. B **16**, 1699 (1977).
[16]B. E. I. Rashba and M. D. Sturge, *Excitons* (North-Holland, Amsterdam, 1982), Chaps. 3 and 4.
[17]W. C. Tait and R. L. Weiher, Phys. Rev. **166**, 769 (1968).
[18]T. Takagahara, Phys. Rev. B **31**, 8171 (1985).
[19]K.-H. Pantke and I. Broser, Phys. Rev. B **48**, 11752 (1993).
[20]J. J. Hopfield and D. G. Thomas, J. Phys. Chem. Solids **12**, 276 (1960).
[21]D. D. Sell, S. E. Stokowski, R. Dingle, and J. V. DiLorenzo, Phys. Rev. B **7**, 4568 (1973).
[22]S. L. Shi and S. J. Xu, J. Appl. Phys. **109**, 053510 (2011).
[23]J. J. Hopfield and D. G. Thomas, Phys. Rev. **132**, 563 (1963).
[24]Y. P. Varshni, Physica **34**, 149 (1967).
[25]J. W. Li, S. Z. Ma, X. J. Liu, Z. F. Zhou, and C. Q. Sun, Chem. Rev. **112**, 2833 (2012).
[26]C. Klingshirn, R. Hauschild, J. Fallert, and H. Kalt, Phys. Rev. B **75**, 115203 (2007).